Performance optimization of a PEM hydrogen-oxygen fuel cell

Maher A.R. Sadiq Al-Baghdadi

Fuel Cell Research Center, International Energy & Environment Foundation, Al-Najaf, P.O.Box 39, Iraq.

Abstract
The objective was to develop a semi-empirical model that would simulate the performance of proton exchange membrane (PEM) fuel cells without extensive calculations. A fuel cell mathematical module has been designed and constructed to determine the performance of a PEM fuel cell. The influence of some operating parameters on the performance of PEM fuel cell has been investigated using pure hydrogen on the anode side and oxygen on the cathode side. The present model can be used to investigate the influence of process variables for design optimization of fuel cells, stacks, and complete fuel cell power system. The possible mechanisms of the parameter effects and their interrelationships are discussed. In order to assess the validity of the developed model a real PEM fuel cell system has been used to generate experimental data. The comparison shows good agreements between the modelling results and the experimental data. The model is shown a very useful for estimating the performance of PEM fuel cell stacks and optimization of fuel cell system integration and operation.
Copyright © 2013 International Energy and Environment Foundation - All rights reserved.

Keywords: PEM fuel cells; Semi-empirical model; Performance; Hydrogen.

1. Introduction
The need of reducing pollutant emissions and of utilising more efficiently the available energy resources (in particular fossil resources) has caused, in recent years, an ever-increasing attention towards fuel cells. In fact, their high conversion efficiency and low environmental impact make them good candidates for substituting, at least in some applications, more conventional conversion systems. Fuel cell technology is expected to play an important role in meeting the growing demand for distributed generation. In an ongoing effort to meet increasing energy demand and also to preserve the global environment, the development of energy systems with readily available fuels, high efficiency and minimal environmental impact is urgently required. A fuel cell system is expected to meet such demands because it is a chemical power generation device, which converts the chemical energy of a clean fuel (e.g. Hydrogen) directly into electrical energy. Still a maturing technology, fuel cell technology has already indicated its advantages, such as its high-energy conversion efficiency, modular design and very low environmental intrusion, over conventional power generation equipment. Among all kinds of fuel cells, proton exchange membrane fuel cells (PEMFCs) are compact and lightweight, work at low temperatures with a high output power density, and offer superior system start-up and shutdown performance. These advantages have sparked development efforts in various quarters of industry to open up new field of applications for PEMFCs, including transportation power supplies, compact cogeneration stationary power supplies, portable power supplies, and emergency and disaster backup power supplies [1-6].

The performance of PEM fuel cells is known to be influenced by many parameters, such as operating temperature, pressure and discharge current. In order to improve fuel cell performances, it is essential to understand these parametric effects on fuel cell operations. To understand and improve the performance of PEMFCs, researchers have developed several mathematical models [7-19] to explain the behaviour of potential variation with the discharge current. Mathematical modelling is a powerful tool for improving the performance of fuel cell stacks. Two main modelling approaches can be found in the literature. The first approach includes mechanistic models, which aim to simulate the heat, mass transfer and electrochemical phenomena encountered in fuel cells. The second approach includes models that are based on semi-empirical equations, which are applied to predict the effect of different input parameters on the voltage–current characteristics of the fuel cell, without examining in depth the physical and electrochemical phenomena involved in fuel cell operation.

Semi-empirical modelling combines theoretically derived differential and algebraic equations with empirically determined relationships. Empirical relationships are employed when the physical phenomena are difficult to be modelled or the theory governing the phenomena is not well understood. Semi-empirical models are, however, limited to a narrow corridor of operating conditions. They cannot accurately predict performance outside of that range. They are very useful for making quick predictions for designs that already exists. They cannot be used to predict the performance of innovative designs, or the response of the fuel cell to parameter changes outside of the conditions under which the empirical relationships were developed. Empirical relationships also do not provide an adequate physical understanding of the phenomena inside the cell. They only correlate output with input. Semi-empirical models are very useful for estimating the performance of PEM fuel cell stacks and optimization of fuel cell system integration and operation.

The aim of this research is to design and construct a mathematical model for investigating the performance of a PEM fuel cell at different operation variables to optimize its performance by changing some of its parameters. Model validation against the experimental data is presented.

2. Background

The fundamental structure of a PEM fuel cell can be described as two electrodes (anode and cathode) separated by a solid membrane acting as an electrolyte (Figure 1). Hydrogen fuel flows through a network of channels to the anode, where it dissociates into protons that, in turn, flow through the membrane to the cathode and electrons that are collected as electrical current by an external circuit linking the two electrodes. The oxygen flows through a similar network of channels to the cathode where oxygen combines with the electrons in the external circuit and the protons flowing through the membrane, thus producing water. The chemical reactions occurring at the anode and cathode electrode of a PEM fuel cell are as follows:

Anode reaction: $H_2 \rightarrow 2H^+ + 2e^-$

Cathode reaction: $\dfrac{1}{2}O_2 + 2H^+ + 2e^- \rightarrow H_2O$

Total cell reaction: $H_2 + \dfrac{1}{2}O_2 \rightarrow H_2O$
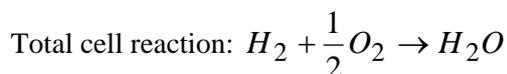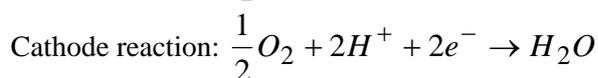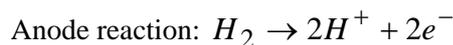
The products of this process are water, DC electricity and heat.

3. Mathematical Model

Useful work (electrical energy) is obtained from a fuel cell only when a current is drawn, but the actual cell potential (V_{cell}) is decreased from its equilibrium thermodynamic potential (E) because of irreversible losses. When current flows, a deviation from the thermodynamic potential occurs corresponding to the electrical work performed by the cell. The deviation from the equilibrium value is called the over potential and has been given the symbol (η). The over potentials originate primary from activation over potential (η_{act}), ohmic over potential (η_{ohmic}) and diffusion over potential (η_{diff}).

Therefore, the expression of the voltage for a single cell is:

$$V_{cell} = E + \eta_{act} + \eta_{ohmic} + \eta_{diff} \qquad (1)$$
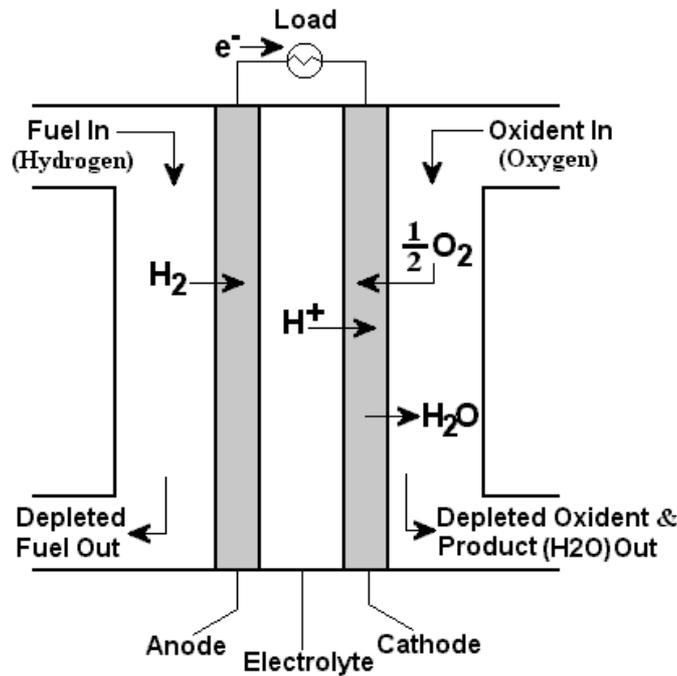
Figure 1: Schematic diagram of a proton exchange membrane fuel cell

The reversible thermodynamic potential of the H2+O2 reaction previously described is given by the Nernst equation:

$$E = E_O + \frac{RT}{zF} \ln\left[P_{H_2}^* \left(P_{O_2}^*\right)^{0.5} \right] \tag{2}$$

where E0 is a reference potential and the partial pressure terms are related to the hydrogen and oxygen concentrations at the anode and cathode. Further expansion of this equation return [7, 8]:

$$E = 1.229 - 0.85 \times 10^{-3} \cdot (T - 298.15) + 4.3085 \times 10^{-5} \cdot T \cdot \left[\ln\left(P_{H_2}^*\right) + \frac{1}{2} \cdot \ln\left(P_{O_2}^*\right) \right] \tag{3}$$

Activation overpotential arises from the kinetics of charge transfer reaction across the electrode-electrolyte interface. In other words, a portion of the electrode potential is lost in driving the electron transfer reaction. Activation overpotential is directly related to the nature of the electrochemical reactions and represents the magnitude of activation energy, when the reaction propagates at the rate demanded by the current.

The activation overpotential can be divided into the anode and cathode overpotentials. The equation for the anode overpotential is [7-9]:

$$\eta_{act,a} = -\frac{\Delta G_{ec}}{2F} + \frac{RT}{2F} \ln\left(4FAk_a^0 C_{H_2}^*\right) - \frac{RT}{2F} \ln(i) \tag{4}$$

The respective equation used for calculating the cathode overpotential is:

$$\eta_{act,c} = \frac{RT}{a_c zF} \left[\ln\left(zFAk_c^0 \exp\left(\frac{-\Delta G_e}{RT}\right) \left(C_{O_2}^*\right)^{(1-a_c)} \left(C_{H^+}^*\right)^{(1-a_c)} \left(C_{H_2O}^*\right)^{a_c} \right) - \ln(i) \right] \tag{5}$$

where z=1 is the number of equivalents involved in the cathode reaction.

In order to have a single expression of the activation overpotential, Eqs. (4) and (5) can be combined and written in a parametric form as follows:

$$\eta_{act} = \xi_1 + \xi_2 T + \xi_3 T \left[\ln(C_{O_2}^*)\right] + \xi_4 T \left[\ln(i)\right]$$

(6)

where the terms ξ_i are semi-empirical coefficients, defined by the following equations:

$$\xi_1 = \left(\frac{-\Delta G_e}{a_c zF}\right) + \left(\frac{-\Delta G_{ec}}{2F}\right)$$

(7)

$$\xi_2 = \frac{R}{a_c zF} \ln\left[zFAk_c^0 \left(C_{H^+}^*\right)^{(1-a_c)} \left(C_{H_2O}^*\right)^{a_c}\right] + \frac{R}{2F}\left[\ln\left(4FAk_a^0 C_{H_2}^*\right)\right]$$

(8)

$$\xi_3 = \frac{R}{a_c zF}(1 - a_c)$$

(9)

$$\xi_4 = -\left(\frac{R}{a_c zF} + \frac{R}{2F}\right)$$

(10)

The concentration of dissolved oxygen at the gas/liquid interface can be defined by Henry's Law expression of the form [8]

$$C_{O_2}^* = \frac{P_{O_2}^*}{5.08 \times 10^6 \exp\left(\frac{-498}{T}\right)}$$

(11)

The use of such semi-empirical coefficients gives a significant degree of flexibility when the model is applied to simulate a specific fuel cell stack, as the terms ξ_i can be obtained by a fitting procedure based on the measured polarization curve of the stack. At the same time, these coefficients have a significant mechanistic background. The values used here for the coefficients ξ_i are the ones proposed in Ref. [7] and also with the works of Maxoulis et al. [8] and Fowler et al. [9] and are shown in Table1.
Ohmic overpotential result from electrical resistance losses in the cell. These resistances can be found in practically all fuel cell components: ionic resistance in the membrane, ionic and electronic resistance in the electrodes, and electronic resistance in the gas diffusion backings, bipolar plates and terminal connections. This could be expressed using Ohm's Law equations such as:

$$\eta_{ohmic} = -i.R^{internal}$$

(12)

Table 1: Values for the Constants used in the Activation and Ohmic Overpotential Expressions

ξ_1	-0.9514	γ_1	0.01605
ξ_2	0.00312	γ_2	-3.5×10^{-5}
ξ_3	7.4×10^{-5}	γ_3	8×10^{-6}
ξ_4	-0.000187	$\gamma_4, \gamma_5, \gamma_6$	0

The total internal resistance is a complex function of temperature and current. In the absence of a generally applicable mechanistic equation to calculate $R^{internal}$, it was preferred to represent it by the following equation [8]

$$R^{internal} = \gamma_1 + \gamma_2 T + \gamma_3 i + \gamma_4 Ti + \gamma_5 T^2 + \gamma_6 i^2$$

(13)

The values of γ_i used are shown in Table 1.

Diffusion overpotential is caused by mass transfer limitations on the availability of the reactants near the electrodes. The electrode reactions require a constant supply of reactants in order to sustain the current flow. When the diffusion limitations reduce the availability of a reactant, part of the available reaction energy is used to drive the mass transfer, thus creating a corresponding loss in output voltage. Similar problems can develop if a reaction product accumulates near the electrode surface and obstructs the diffusion paths or dilutes the reactants. As proposed by Berning et al. [10], Chahine et al. [11], and Hamelin et al. [12], the total diffusion overpotential can be represented by the following expression:

$$\eta_{diff} = m \exp(n\,i) \tag{14}$$

The diffusion overpotential is directly related to the concentration drop of reactant gases, and thus inversely to the growth rate n of by-products of the electrochemical reaction in the catalyst layers, flow fields, and across the electrode. A physical interpretation for the parameters m and n was not given, but Berning et al. [10] found in their study that m correlates to the electrolyte conductivity and n to the porosity of the gas diffusion layer. Both m and n relate to water management issues. A partially dehydrated electrolyte membrane leads to a decrease in conductivity, which can be represented by m, whereas an excess in liquid water leads to a reduction in porosity and hence to an early onset of mass transport limitations, which can be captured by the parameter n.

The mass transfer coefficient m decreases linearly with cell temperature but it has two dramatically different slopes as shown by the following expressions [11];

$$m = 1.1 \times 10^{-4} - 1.2 \times 10^{-6}(T - 273.15) \qquad \text{for } T \geq 312.15\,K\,(39\,^{\circ}C) \tag{15}$$

$$m = 3.3 \times 10^{-3} - 8.2 \times 10^{-5}(T - 273.15) \qquad \text{for } T < 312.15\,K\,(39\,^{\circ}C) \tag{16}$$

The thermodynamic efficiency of the fuel cell E_{fc} can be determined as the ratio of output work rate W_{gross} to the product of the hydrogen consumption rate $\dot{m}_{H_2}$ and the lower heating value of hydrogen LHV_{H_2} [13].

$$E_{fc} = \frac{W_{gross}}{\dot{m}_{H_2}.LHV_{H_2}} \tag{17}$$

Once the output voltage of the stack is determined for a given output current, the gross output power is found as:

$$W_{gross} = I.V_{cell} \tag{18}$$

The output current is correlated with the hydrogen mass flow rate by the equation [13];

$$\dot{m}_{H_2} = \frac{I.MW_{H_2}}{2F} \tag{19}$$

Thus, the thermodynamic efficiency of the fuel cell can simplifies as follows;

$$E_{fc} = \frac{2V_{cell}F}{MW_{H_2} \cdot LHV_{H_2}} \tag{20}$$

4. Results and discussion
Model validation involves the comparison of model results with experimental data, primarily for the purpose of establishing confidence in the model. To validate the mathematical model presented in the preceding section, comparisons were made to the experimental data for a single cell operated at temperature of 40 C, 1 atm anode pressure (H_2) and 1 atm cathode pressure (O_2), (Figure 2).
Figure 3 compares the computed polarization curves with the measured ones. The calculated curve shows good agreement with the experimental data.
The resulting inlet gas composition of the cathode side gas stream for different pressures is shown in Figure 4. Clearly, at an operation pressure of 1 atm the effect of the temperature on the inlet composition

is much stronger than at elevated pressures. At 80 oC for 1 atm pressure, almost 46% (molar) of the incoming cathode side gas stream consists of water vapor and only around 54% is oxygen. It was already noted in Figure 4 that the change in the inlet gas composition is particularly strong in the range from 1 to 3 atm. Above 3 atm the composition changes only slightly with the pressure.

Figures 5 and 6 show the efficiency-power density-cell potential relationship. The performance of the fuel cell increases with the increase of the cell temperature. The exchange current density increases with the increase of fuel cell temperature, which reduces activation losses. Another reason for the improved performances is that higher temperatures improve mass transfer within the fuel cells and results in a net decrease in cell resistance (as the temperature increases the electronic conduction in metals decreases but the ionic conduction in the electrolyte increases). This may explain the improvement of the performance [3]. The shifting of the polarization curves towards higher voltage at higher current densities when increasing the cell temperature is due to the increase of conductivity of the membrane.

The performance of the fuel cell is improved with the increase of pressure. The higher open circuit voltage at the higher pressures can be explained by the Nernst equation. The overall polarization curves shift positively as the pressure increases. Another reason for the improved performances is the partial pressure increase of the reactant gases with increasing operating pressure (cf. Figure 4).

The fuel cell efficiency is directly proportional to the cell potential, as shown in equation (20); therefore, the efficiency is also a function of power density. Figures 5 and 6, therefore, have both voltage and efficiency on the "y" axis. The efficiency at maximum power is much lower than the efficiency at partial loads, which makes the fuel cells very attractive and efficient for applications with highly variable loads where most of the time the fuel cell is operated at low load and high efficiency. The fuel cell nominal efficiency is therefore an arbitrary value, ranging anywhere between 0.3 and ~ 0.65, which can be selected for any fuel cell based on economic rather than physical constraints. For example, for a fuel cell at a reactant pressures of 1 atm and 65 C cell temperature, one may select a maximum operating point at 0.425 V and 1.258 A resulting in 0.535 W and an efficiency of 0.41. However, one may get the same power output by selecting two cells, connected in series, operating at 0.67 V and 0.4 A each. Obviously, the latter would be twice as expensive, but it would be more efficient (0.58), and therefore would consume less fuel. This example clearly illustrates that the efficiency of a fuel cell may be "bought" by adding more cells, and it is driven by economic factors, such as the cost of individual cells, cost of hydrogen and the resulting cost of generated power.

Return to Figs. 5 and 6, the maximum power occurs at approximately 0.3 to 0.6 V, which corresponds to relatively high current. At the peak point, the internal resistance of the cell is equal to the electrical resistance of the external circuit. However, since efficiency drops with increasing voltage, there is a tradeoff between high power and high efficiency. Fuel cell system designers must select the desired operating range according to whether efficiency or power is paramount for the given application.

Figure 2. A single PEM fuel cell testing hardware
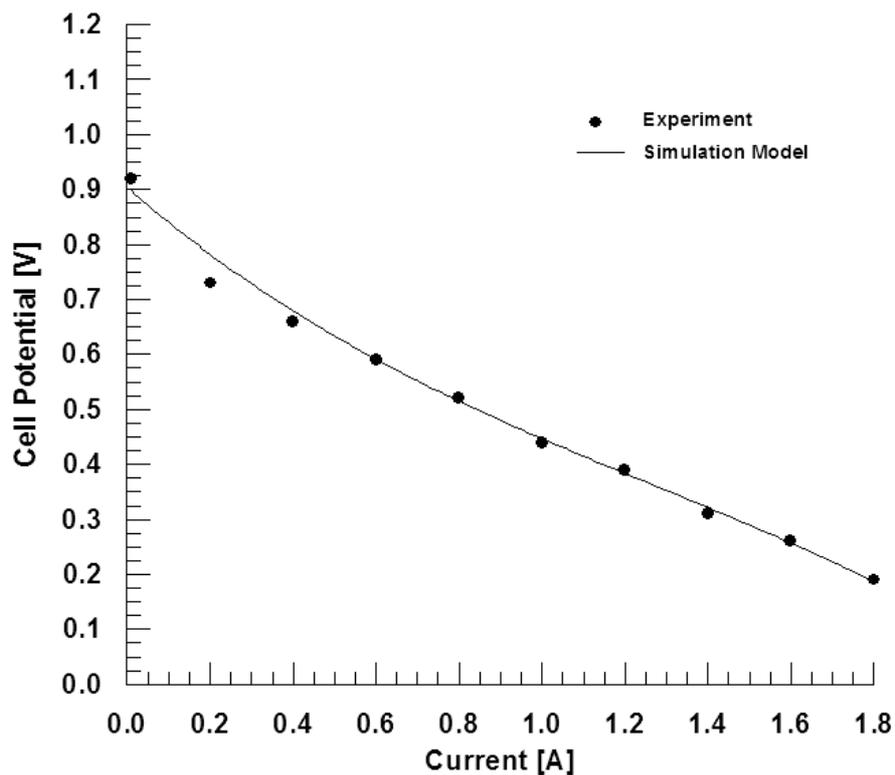
Figure 3: Comparison between the model predictions and experimental results
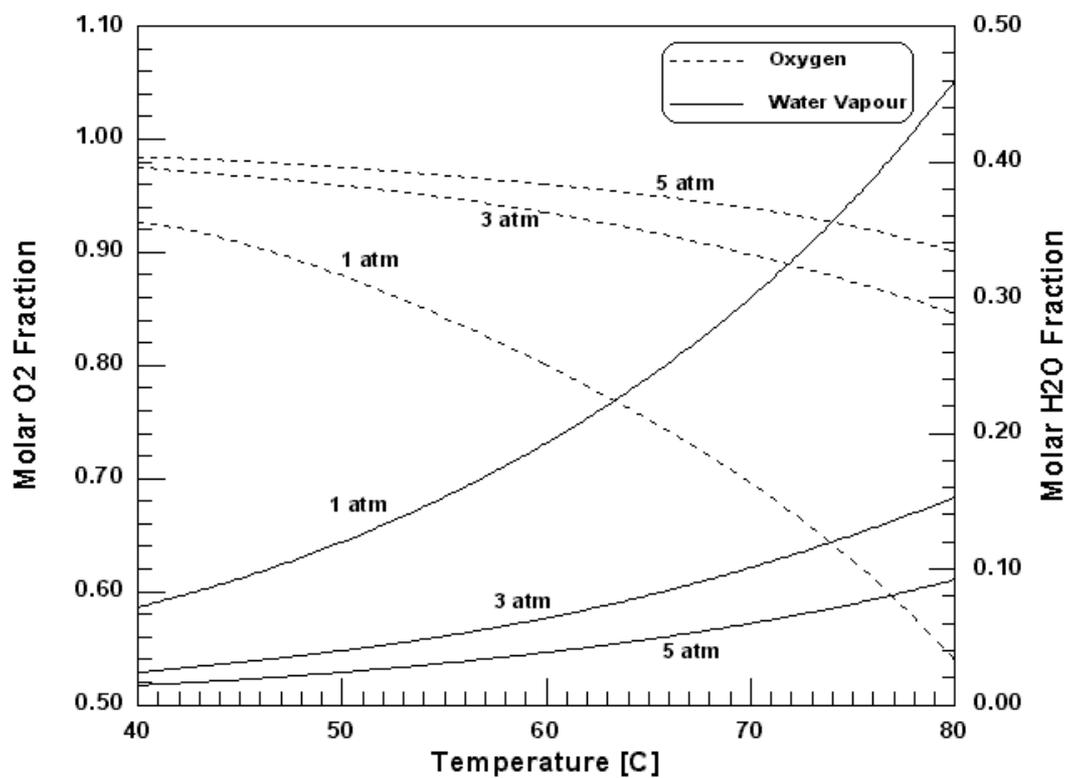
Figure 4: Molar inlet composition of the cathode side gas stream as function of temperature and different values of reactant pressures
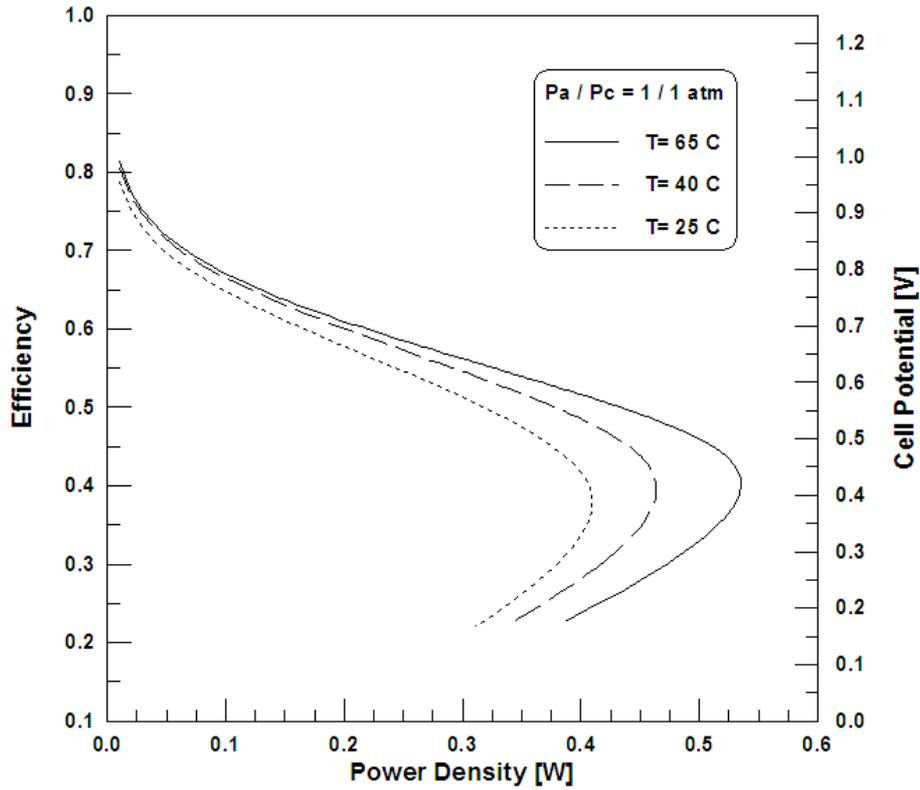
Figure 5: Relationship between fuel cell efficiency and power output for different values of cell temperature
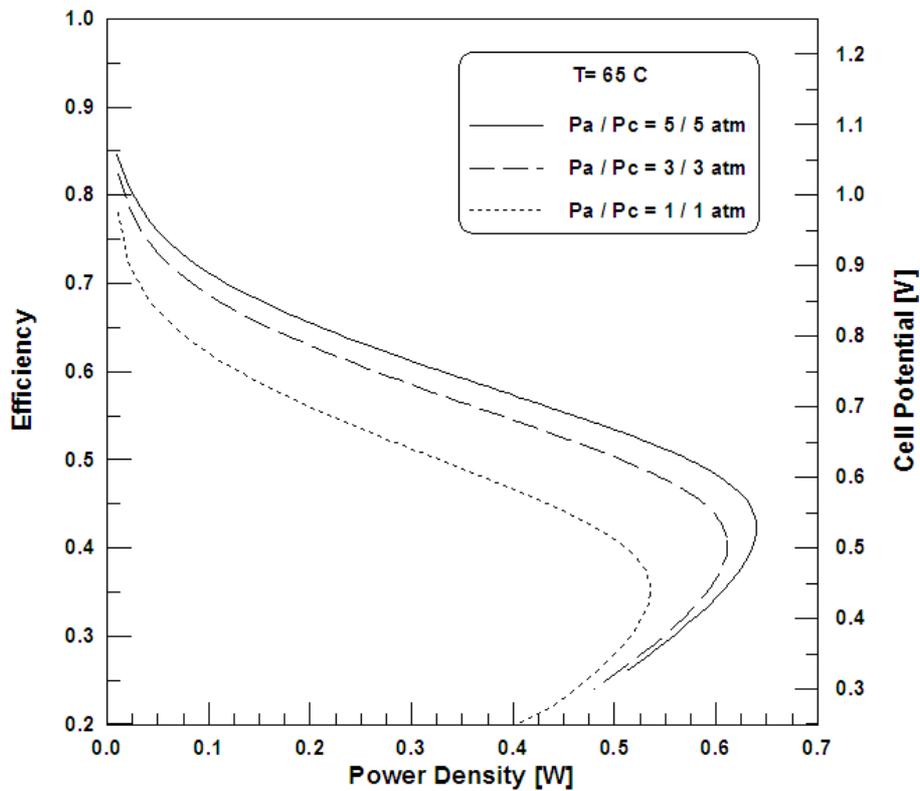
Figure 6: Relationship between fuel cell efficiency and power output for different values of reactant pressures

5. Conclusion

A semi-empirical model of a PEM fuel cell has been developed and the effect of operation conditions on the cell performance has been investigated. The objective was to develop a semi-empirical model that would simulate the performance of fuel cells without extensive calculations. The present model can be used to investigate the influence of process variables for design optimization of fuel cells, stacks, and complete fuel cell power system.

The results showed that the effect of the temperature on the inlet gas composition is particularly strong in the range from 1 to 3 atm. Above 3 atm the composition changes only slightly with the pressure. Changes in operating pressure have a large impact on the inlet composition and, hence, on the fuel cell performance. For most applications, and particularly for steady operation, a fuel cell does not have to be operated at its maximum power, where the efficiency is the lowest. When higher nominal cell potential is selected, the cost of additional cells is offset by savings on fuel cost. The results of the present study that indicate the operating temperature and pressure can be optimized, based on cell performance, for a given design and other operating conditions.

Nomenclature

A	active cell area (cm^2)
a_c	chemical activity parameter for the cathode
$C_{H^+}^*$	proton concentration at the cathode membrane / gas interface (mol/cm^3)
$C_{H_2}^*$	liquid phase concentration of hydrogen at anode / gas interface (mol/cm^3)
$C_{H_2O}^*$	water concentration at the cathode membrane / gas interface (mol/cm^3)
$C_{O_2}^*$	oxygen concentration at the cathode membrane / gas interface (mol/cm^3)
E	thermodynamic potential (V)
E_{fc}	thermodynamic efficiency
F	Faraday's constant (96487 C/mol)
i	current density (A/cm^2)
I	current (A)
k_a^0, k_c^0	intrinsic rate constant for the anode and cathode reactions, respectively (cm/s)
LHV_{H_2}	lower heating value of hydrogen (J/kg)
m, n	mass transfer coefficients
$\dot{m}_{H_2}$	hydrogen mass flow rate (kg/s)
MW_{H_2}	molecular mass of hydrogen (kg/mol)
P_a, P_c	total pressure of anode and cathode, respectively (atm)
$P_{H_2}^*$, $P_{O_2}^*$	partial pressure of hydrogen and oxygen at the anode catalyst / gas interface and cathode catalyst / gas interface, respectively (atm)
R	gas constant (8.314 J/mol K)
$R^{internal}$	total internal resistance ($\Omega\,cm^2$)
T	cell temperature (K)
V_{cell}	cell voltage (V)
W_{gross}	gross output power (W)
ΔG_e	standard state free energy of the cathode reaction (J/mol)
ΔG_{ec}	standard state free energy of chemisorption from the gas state (J/mol)

Greek letters

η_{act}	activation over potential

η_{diff}	diffusion over potential
η_{ohmic}	ohmic over potential
$\gamma_1, \gamma_2, \gamma_3, \gamma_4$	semi-empirical coefficients for calculation of ohmic overpotential
$\xi_1, \xi_2, \xi_3, \xi_4$	semi-empirical coefficients for calculation of activation overpotential

References

[1]   T. Susai, M.Kaneko, K. Nakato, T. Isono, A. Hamada and Y. Miyake, Optimization of proton membranes and the humidifying conditions to improve cell performance for polymer electrolyte fuel cells. Int J Hydrogen Energy 2001;26(6):631-637

[2]   F. Barbir and T. Gomez, Efficiency and economics of proton exchange membrane (PEM) fuel cells. Int J Hydrogen Energy 1997;22(10-11):1027-1037

[3]   Lin Wang, Attila Husar, Tianhong Zhou and Hongtan Liu, A parametric study of PEM fuel cell performances. Int J Hydrogen Energy 2003;28(11):1263-1272

[4]   R. Johnson, , C. Morgan, D. Witmer and T. Johnson, Performance of a proton exchange membrane fuel cell stack. Int J Hydrogen Energy 2001;26(8):879-887

[5]   S. E. Wright, Comparison of the theoretical performance potential of fuel cells and heat engines. Renewable Energy 2004;29(2):179-195

[6]   K.S. Dhathathreyan, P. Sridhar, G. Sasikumar, K.K. Ghosh, G. Velayutham, N. Rajalakshmi, C.K. Subramaniam, M. Raja and K. Ramya, Development of polymer electrolyte membrane fuel cell stack. Int J Hydrogen Energy 1999;24(11):1107-1115

[7]   Ronald F. Mann, John C. Amphlett, Michael A. I. Hooper, Heidi M. Jensen, Brant A. Peppley and Pierre R. Roberge, Development and application of a generalised steady-state electrochemical model for a PEM fuel cell. J Power Sources 2000;86(1-2):173-180

[8]   Christos N. Maxoulis, Dimitrios N. Tsinoglou and Grigorios C. Koltsakis, Modeling of automotive fuel cell operation in driving cycles. Energy Conversion and Management 2004;45(4):559-573

[9]   Michael W. Fowler, , Ronald F. Mann, John C. Amphlett, Brant A. Peppley and Pierre R. Roberge, Incorporation of voltage degradation into a generalised steady state electrochemical model for a PEM fuel cell. J Power Sources 2002;106(1-2):274-283

[10] T. Berning and N. Djilali, Three-dimensional computational analysis of transport phenomena in a PEM fuel cell—a parametric study. J Power Sources 2003;124(2):440-452

[11] R. Chahine, F. Laurencelle, J. Hamelin, K. Agbossou, M. Fournier, T.K. Bose and A. Laperriere, Characterization of a Ballard MK5-E Proton Exchange Membrane Fuel Cell Stack. Fuel cells 2001;1(1):66-71

[12] J. Hamelin, K. Agbossou, A. Laperriere and T.K. Bose, Dynamic behavior of a PEM fuel cell stack for stationary applications. Int J Hydrogen Energy 2001;26(6):625-629

[13] R. Cownden, M. Nahon and M.A. Rosen, Modelling and analysis of a solid polymer fuel cell system for transportation applications. Int J Hydrogen Energy 2001;26(6):615-623

[14] C.R. Derouin, E.A. Ticianelli, S. Srinivasan, Localization of platinum in low catalyst loading electrodes to attain high power densities in SPE fuel cells. J. Electroanal. Chem. 1998;251(2):275-295

[15] Sampath Yerramalla, Asad Davari, Ali Feliachi and Tamal Biswas, Modeling and simulation of the dynamic behavior of a polymer electrolyte membrane fuel cell. J Power Sources 2003;124(1):104-113

[16] M. Ceraolo, C. Miulli and A. Pozio, Modelling static and dynamic behaviour of proton exchange membrane fuel cells on the basis of electro-chemical description. J Power Sources 2003;113(1):131-144

[17] M. R. von Spakovsky, and B. Olsommer, Fuel cell systems and system modeling and analysis perspectives for fuel cell development. Energy Conversion and Management 2002;43(9-12):1249-1257

[18] J. C. Amphlett, R. F. Mann, B. A. Peppley, P. R. Roberge and A. Rodrigues, A model predicting transient responses of proton exchange membrane fuel cells. J Power Sources 1996;61(1-2):183-188

[19] N.P. Siegel, M.W. Ellis, , D.J. Nelson and M.R.von Spakovsky, Single domain PEMFC model based on agglomerate catalyst geometry. J Power Sources 2003;115(1):81-89